Geotechnical Testing Journal, Vol. 35, No. 6, 2012
Available online at www.astm.org
doi:10.1520/GTJ20120083

Mahdi Rojhani,[1] *Majid Moradi,*[2] *Mohammad Hossein Ebrahimi,*[3] *Abbas Galandarzadeh,*[4] *and Shiro Takada*[5]

Recent Developments in Faulting Simulators for Geotechnical Centrifuges

REFERENCE: Rojhani, Mahdi, Moradi, Majid, Ebrahimi, Mohammad Hossein, Galandarzadeh, Abbas, and Takada, Shiro, "Recent Developments in Faulting Simulators for Geotechnical Centrifuges," *Geotechnical Testing Journal*, Vol. 35, No. 6, 2012, pp. 1–11, doi:10.1520/GTJ20120083. ISSN 0149-6115.

ABSTRACT: In addition to the dynamic effects of faulting that cause earthquake wave propagation, large-scale deformation of faulting is a hazard for structures near the fault. Analytical and numerical studies have been conducted on fault rupture propagation through soil deposits and soil-structure interactions such as buried pipelines and buildings. However, evaluating the results is difficult because well-documented field case histories are limited. Researchers resort to physical modeling and laboratory tests to address this deficiency. Because full-scale modeling is time consuming and costly, centrifuge modeling is the best option. The first step for centrifuge modeling of faulting is to design and manufacture a fault simulator in a centrifuge. In this paper, all available information about fault simulators worldwide is presented as an archive for researchers. A detailed report on the design and manufacture of the new fault simulator at the Univ. of Tehran is also presented and the testing of a simulated buried continuous pipeline subjected to normal and reverses faulting is discussed. The fault simulator results were shown to correspond to natural faulting deformation.

KEYWORDS: earthquake, permanent ground deformation, centrifuge models, faulting, fault simulator

Nomenclature

C_C = coefficient of curvature
C_u = coefficient of uniformity
D = pipe outer diameter
D_{50} = average particle size of sand backfill
e_{max} = maximum void ratio
e_{min} = minimum void ratio
FC = fine content of soil
G_s = specific gravity of soil particle
H = depth of soil from surface to top of pipe
t = pipe wall thickness
α = pipeline fault orientation angle
β = fault deformation (dip) angle

Manuscript received September 18, 2010; accepted for publication June 6, 2012; published online September 2012.

[1]Ph.D. candidate, Dept. of Soil Mechanics and Foundation Engineering, School of Civil Engineering, Univ. of Tehran, 11365/4563 Tehran, Iran, e-mail: mrojhani@ut.ac.ir
[2]Assistant Professor, Dept. of Soil Mechanics and Foundation Engineering, School of Civil Engineering, Univ. of Tehran, 11365/4563 Tehran, Iran, e-mail: mmoradi@ut.ac.ir
[3]Mechanical engineer, e-mail: mh_ebr@yahoo.com
[4]Assistant Professor, Dept. of Soil Mechanics and Foundation Engineering, School of Civil Engineering, Univ. of Tehran, 11365/4563 Tehran, Iran, e-mail: aghaland@ut.ac.ir
[5]Adjunct Professor, Dept. of Soil Mechanics and Foundation Engineering, School of Civil Engineering, Univ. of Tehran, 11365/4563 Tehran, Iran, e-mail: takada@lifeline-eng.com

Introduction

Geotechnical seismic hazards can be broadly classified into wave propagation hazards and permanent ground deformation (PGD) hazards. Wave propagation damage occurs over very large areas, but with low maximum strain limits or damage rates. However, PGD damage typically occurs in isolated areas with high damage rates. Wave propagation hazards are characterized by a transient strain in the ground caused by traveling wave effects. PGD hazards (such as faulting, landslides, seismic settlement, and lateral spreading due to liquefaction) are characterized by many factors, including their geometry and the amount of deformation in the PGD zone.

Although avoiding construction in an area susceptible to PGD is the best solution, such construction is often inevitable. Thus, research about PGD, its causes and effects is necessary using analytical, numerical and experimental studies. However, analytical and numerical studies conducted on faulting should ideally be verified by field case histories. The lack of validated field case histories suggests that the results of physical modeling tests should be used for this purpose (Choo et al. 2007).

Centrifuge modeling is the latest physical modeling technique. The centrifuge technique is considered the best available means to simulate prototype conditions in geotechnics (Simpson and Tatsuoka 2008). This paper presents the results of research on the design and manufacture of equipment for simulating faulting using the centrifuge technique. Although a number of fault simulators have been built by researchers (O'Rourke et al. 2003, Lee 2005, Bransby et al. 2008), there are no published, comprehensive details of their experiments and apparatuses. The present paper addresses these available experiments.

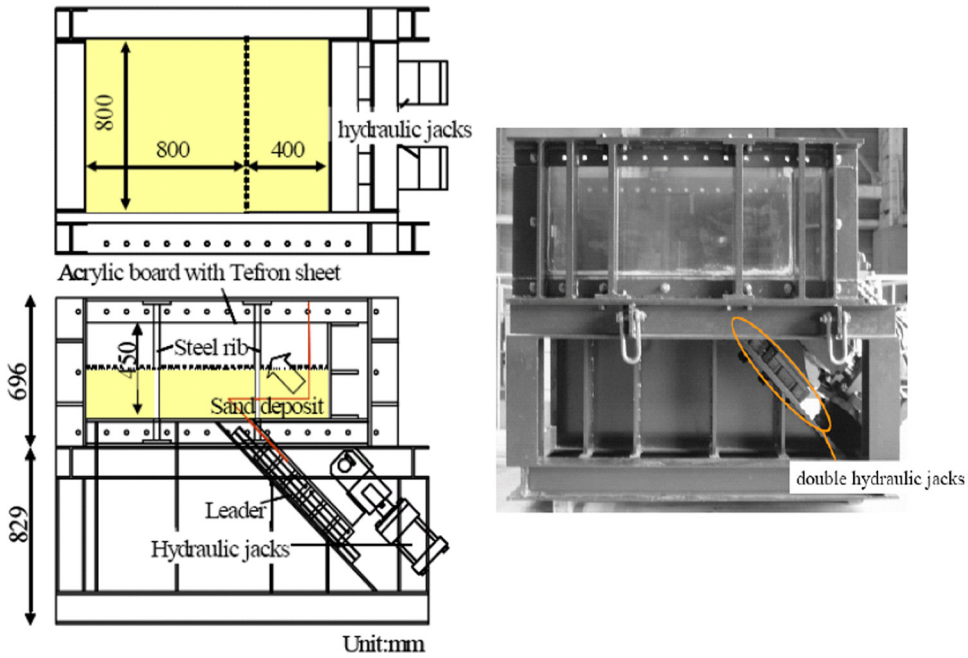

FIG. 1—*Waseda Univ. fault simulator (Lee and Hamada 2005).*

Fault Simulators Worldwide

The Lee and Hamada (2005) testing apparatus for centrifuge modeling was constructed by Waseda Univ. with a steel frame and consisted of 30-mm-thick steel plates and an acrylic board with a thickness of 50 mm on one side of the box. The dimensions of the apparatus were 1.2 m × 0.8 m × 0.45 m (length, width, depth). Part of the testing box could be moved up or down along a fixed dip angle (45°) relative to the fixed part to simulate normal or reverse faulting. Lee's box (Fig. 1) had double 2.0 MN capacity hydraulic jacks. A Teflon sheet was used between the soil specimen and each side wall of the apparatus to minimize frictional resistance. This simulator was equipped with remote-controlled hydraulic jacks and a remote-controlled video camera to observe the deformation of the surface of the ground model. The purpose of the research was to study earthquake fault rupture propagation.

Another apparatus constructed to simulate faults is shown in Fig. 2 (El Nahas et al. 2006). This apparatus was developed by Bransby et al. (2008) at the Univ. of Dundee to simulate normal and reverse faulting in a centrifuge. The study investigated fault rupture propagation through sand and its interaction with strip footings. This simulator was contained within a centrifuge strong box with internal dimensions of 800 m × 500 mm × 500 mm (length, width, depth). The strong box contained front and back transparent Perspex plates through which the models were monitored in flight. The soil container of the simulator had inside dimensions of 655.9 mm × 500 mm × 220 mm (width, breadth, depth) and consisted of stationary aluminum blocks, a stationary composite steel and concrete block, a movable triangular soil base block and soil retaining plates (Fig. 2). It simulated faulting at the desired dip angle. The model specifications were fulfilled through the use of a central guidance system and three trapezoidal aluminum blocks that were used as a rigid moving base and wall (shaded in Fig. 2). To ensure that the apparatus gave a fixed dip angle, a liner bearing was placed on the left side of the base block (supported by the rigid aluminum blocks supporting the footwall) and an additional three bearings were placed on trapezoidal aluminum blocks connected to the displacing (hanging wall) side wall or soil retaining plate. Two

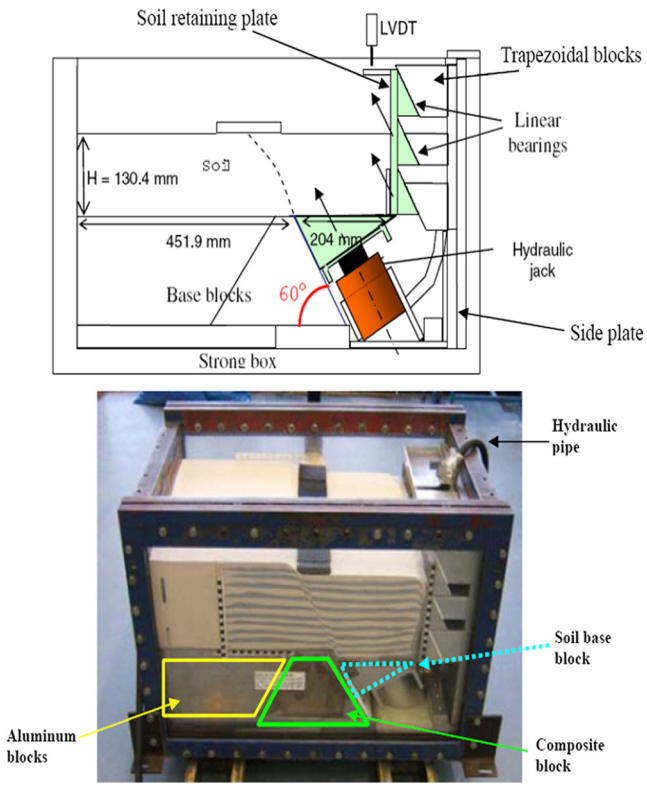

FIG. 2—*Univ. of Dundee fault simulator (El Nahas et al. 2006).*

TABLE 1—*Specifications of two-section split container (Ha et al. 2006).*

Items	Details
Overall dimensions	1270 mm × 1000 mm × 460 mm
Inside container dimensions	1140 mm × 760 mm × 200 mm
Empty weight	2227 N
Horizontal displacement	±40 mm
Vertical displacement	+40 mm
Operating hydraulic pressure	20.7 MPa
Max. dynamic actuator force	8.9 kN
Max. static actuator force	26.7 kN

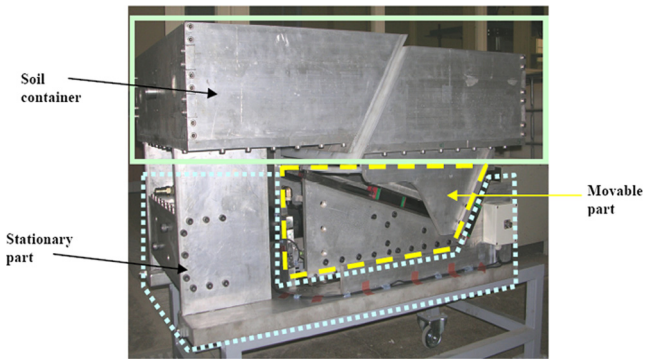

FIG. 3—*Main parts of FSUT-RN60.8 simulator.*

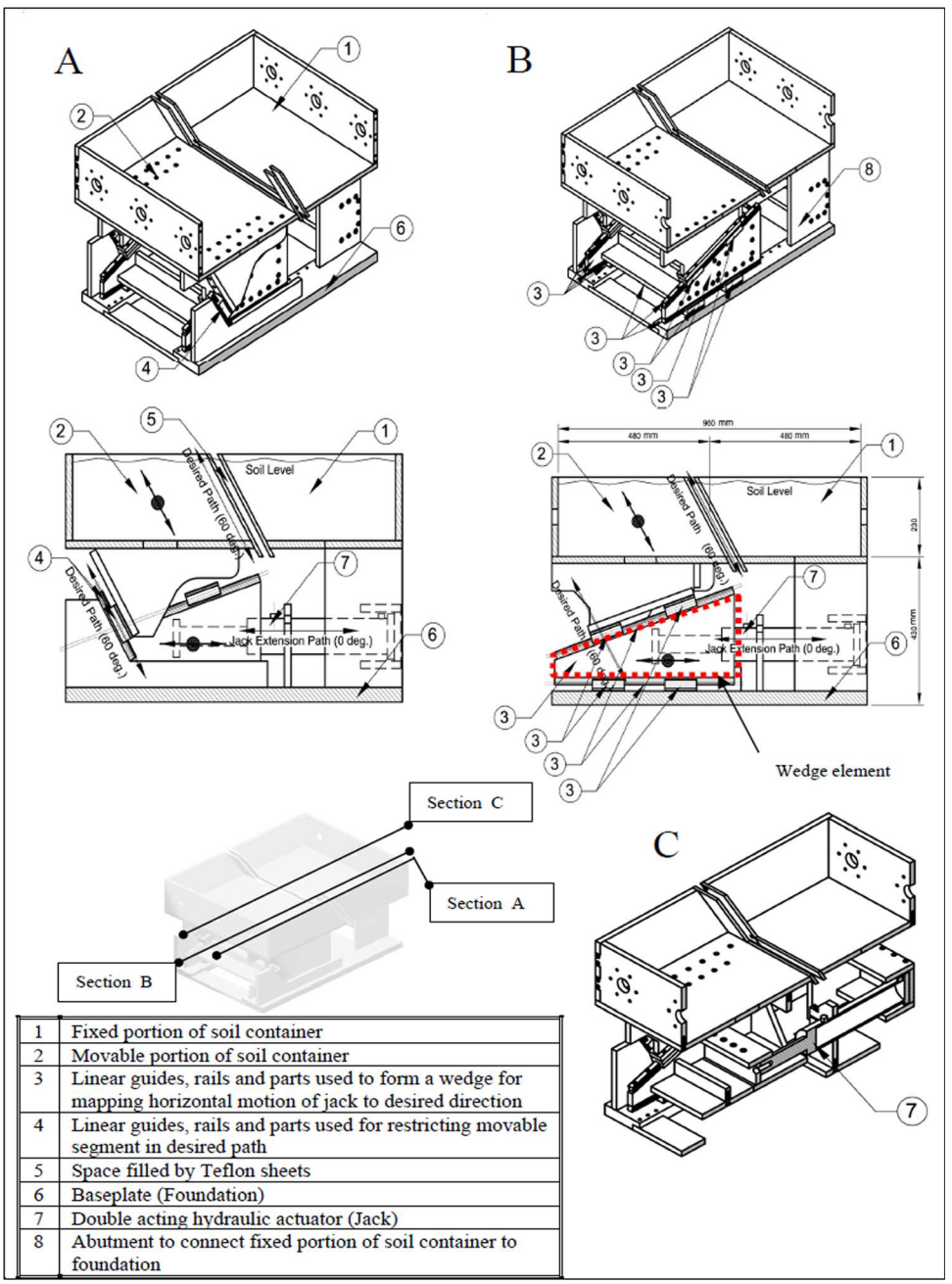

1	Fixed portion of soil container
2	Movable portion of soil container
3	Linear guides, rails and parts used to form a wedge for mapping horizontal motion of jack to desired direction
4	Linear guides, rails and parts used for restricting movable segment in desired path
5	Space filled by Teflon sheets
6	Baseplate (Foundation)
7	Double acting hydraulic actuator (Jack)
8	Abutment to connect fixed portion of soil container to foundation

FIG. 4—*Section drawing of FSUT-RN60.8.*

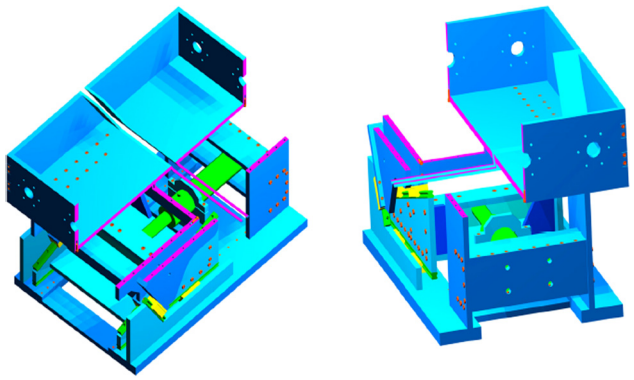

FIG. 5—*Schematic 3D view of FSUT-RN60.8.*

TABLE 2—*Specifications of hydraulic system for FSUT-RN60.8.*

Item	Description
Discharge pressure of power pack	120 bar (*g*)
Minimum design pressure of equipment	200 bar (*g*)
Power pack installation	outside centrifuge hall
Method of hydraulic power transition to container	rotary joints installed on centrifuge rotating axis
Type of actuator	double acting cylinder
Actuator maximum stroke	240 mm
Actuator cylinder diameter	80 mm
Actuator rod diameter	50 mm
Actuator minimum load capacity	50 kN
Load capacity of system in motion direction	150 kN

hydraulic actuators with 300 kN load capacity and a 62 mm stroke were used to push the soil base block of the simulator up or down. The hydraulic actuators rested on a fixed base block attached to the side plate and were connected to an oil pressure gauge (25 MPa), a hydraulic pump, and a non-return valve outside the centrifuge through the hydraulic slip ring. The maximum offset length achievable by this apparatus was 26.4 mm in the normal faulting mode and 33 mm in the reverse faulting mode. All the metal blocks and plates inside the box were made of aluminum alloy 6082T6 (El Nahas et al. 2006). All edges of the simulator were lined with sandpaper to model a fully rough boundary condition (Bransby et al. 2008). PTFE plates (coefficient of friction = 0.1) were bolted on all block and plate surfaces where displacements took place during the tests to reduce the friction forces on them (El Nahas et al. 2006).

O'Rourke constructed a fault simulator at Rensselaer Polytechnic Institute (RPI) in 2003 (O'Rourke et al. 2003) that simulated a strike fault. The simulator had inside dimensions of 1 m × 0.354 m × 0.203 m and consisted of two halves; one fixed and the other movable. The displacement of the movable portion was performed using a 3000 psi hydraulic actuator system. The simulator was controlled remotely by a flow-metering valve and a servo valve controlled the rate of movement and the motion of the actuator. In order to measure the actuator force, a load cell was located between the movable portion and the actuator. The maximum possible offset of the apparatus was 80 mm. To minimize frictional force, the moving portions of the box were supported and guided by roller bearings. The sliding interface between the fixed and movable portions was equipped with low friction Teflon seals protected by steel shields. This apparatus was constructed to study pipeline response due to faulting.

To complement research on the response of buried pipelines to earthquake faulting, O'Rourke constructed a second fault simulator (CMC-SB3) at RPI. The inside dimensions of the new container were 1140 mm × 760 mm × 200 mm. One portion of the two-section split container could be offset horizontally and the other portion vertically. Thus, the split container could simulate strike-slip, normal and reverse faulting and also combinations of them (oblique-slip faulting). The dip angle of the fault was restricted to a right angle. The detailed specifications of CMC-SB3 are presented in Table 1. This apparatus was equipped with a control and feedback processing servo-controller that obtained its input signals from a data acquisition (DAC) system.

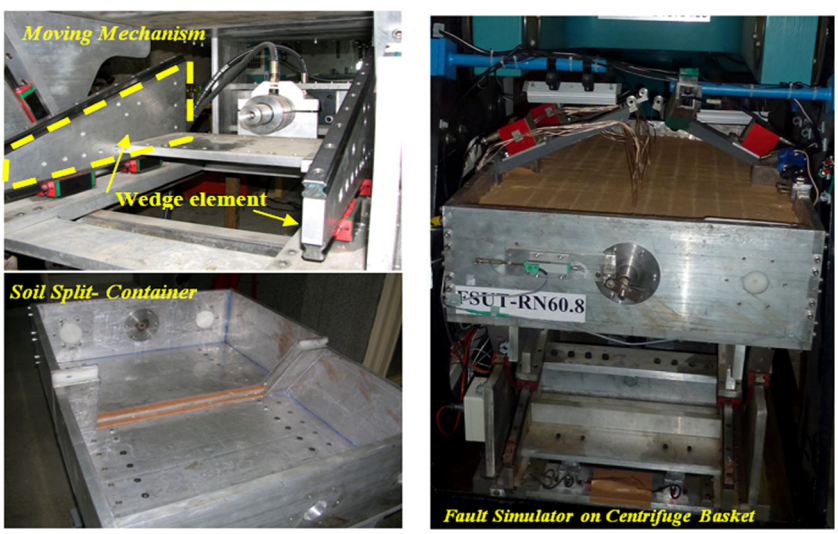

FIG. 6—*FSUT-RN60.8 fault simulator.*

TABLE 3—*Main characteristics of University of Tehran centrifuge.*

Item	Description
Force ($g \times t$)	150
Radius (m)	3
Basket width (m)	0.8
Basket length (m)	1
Basket depth (m)	0.8
Maximum acceleration (g)	130
Maximum load under max. acceleration (N)	8500
Maximum load (N)	15 000
Maximum acceleration under max. load (g)	100

Univ. of Tehran Fault Simulator

The Univ. of Tehran fault simulator and its physical, mechanical, hydraulic, and control systems are described. The results of initial modeling tests are also presented to allow evaluation of the performance of the simulator. These first tests modeled a buried continuous pipeline subject to faulting. The results include soil and pipe deformations and strains induced by normal and reverse faulting in four models.

Physical Properties

The fault simulator at the Univ. of Tehran (FSUT-RN60.8) was designed to simulate normal and reverse faulting in a geotechnical centrifuge at up to 50 g. The overall size of the simulator (FSUT-RN60.8) is 1020 mm × 760 mm × 680 mm (length, width, height) with an empty weight of 2300 N. The FSUT-RN60.8 simulator consists of a stationary part, soil container and movable part (Fig. 3).

The simulator and its accessories are installed on two strong aluminum blocks 150 mm in width, 40 mm in thickness and 1000 mm in length as the foundation (element 6 in Fig. 4) to resist actuator force (horizontal) and substantial vertical force from the weight in Ng gravity acceleration in flight. The other elements are two strong abutments connecting the fixed portion of the soil container to the foundation (element 8 in Fig. 4), a jack back support beam to resist the reaction of the actuator and triangular plates to ensure the fixed dip angle during faulting.

The soil container consists of a fixed portion connected to the foundation on the hanging wall side of the fault (element 1 in Fig. 4) and a movable portion assembled on the movable part on the footwall side (element 2 in Fig. 4). The soil container is 960 mm × 700 mm × 230 mm (length, width, height). The split edge of the box is inclined 30° from the vertical and divides the box at the longest dimension (960 mm). The maximum range of displacement of the container in the direction of motion or fault offset is ±40 mm, which is equivalent to ±2 m on the prototype scale at 50 g of acceleration.

TABLE 4—*Scaling laws for centrifuge testing.*

Parameter	Model\Prototype	Dimensions
Length	1/N	L
Strain	1	1
Stress	1	$ML^{-1}T^{-2}$
Acceleration	N	LT^{-2}
Axial rigidity	$1/N^2$	MLT^{-2}
Flexural rigidity	$1/N^4$	ML^3T^{-2}

TABLE 5—*Summary of test models (all dimensions in prototype scale).*

Test No.	Fault Type	D (m)	t (mm)	D/t	H (m)	H/D	(α^0)	(β^0)	Acc.	Peak offset (m)
1	reverse	.32	16	20	0.88	2.8	60	90	40 g	2.8
2	normal	.32	16	20	0.88	2.8	60	90	40 g	2.3
3	reverse	1	20	50	2	2	60	90	40 g	2.8
4	normal	1	20	50	2	2	60	90	40 g	2.3

A high strength 7075 aluminum alloy material was selected for most parts of FSUT-RN60.8. This was selected to achieve a very rigid, reliable and low weight apparatus. The parts of FSUT-RN60.8 were assembled using bolted connections. On the prototype scale, the maximum offset rate of FSUT-RN 60.8 is 200 mm/s for normal faulting and 300 mm/s for reverse faulting.

Mechanical Properties

A fault simulator operating at 50 g centrifuge must be stable in both portions of the container during the precise motion of the moving segment, which experiences highly unbalanced forces and moments amplified by high acceleration at a constant deformation rate, and maintain a permanent distance between the portions on the sliding plane and a fixed dip angle of deformation during faulting. Forces and moments are caused by the weight of the simulator itself, the weight of the soil, friction at the fault edge and under the test pipe. Another important factor is the need to limit the apparatus dimensions to fit the dimensions of the centrifuge.

FSUT-RN60.8 took the novel step of using a wedge to lift the movable portion of the soil container. The wedge is a triangular tool that can be used to lift an object or hold an object in place (element 3 in Fig. 4). It functions by converting a force applied to its blunt end into forces perpendicular to its inclined surfaces. Pushing a wedge element under the movable soil container causes it to move up and pulling the wedge out from under it moves the container down (Figs. 4–6). This mechanism converts 240 mm of the horizontal motion of the hydraulic actuator into 80 mm of motion in the 60° angle direction. The wedge was equipped with

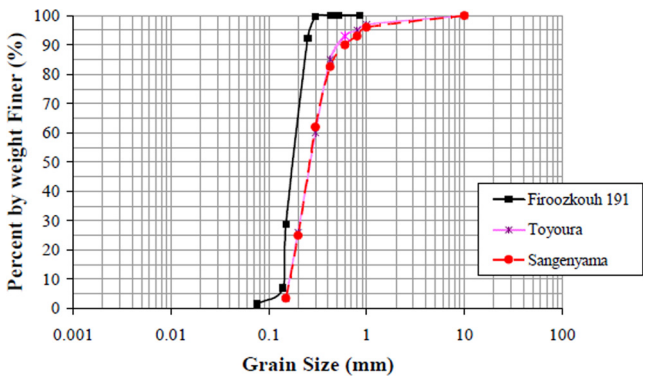

FIG. 7—*Grain size distribution curve of Firoozkouh-191.*

TABLE 6—*Material properties for sand backfill.*

Sand Type	G_s	e_{max}	e_{min}	D_{50} (mm)	FC	C_u	C_c
Firoozkouh-191	2.65	0.894	0.622	0.17	1%	1.27	0.96
Toyoura[a]	2.65	0.977	0.597	0.17	0%	1.54	1.25
Sengenyama[a]	2.72	0.911	0.55	0.27	2.3%	2.15	1.21

[a]Ghalandarzadeh 1997.

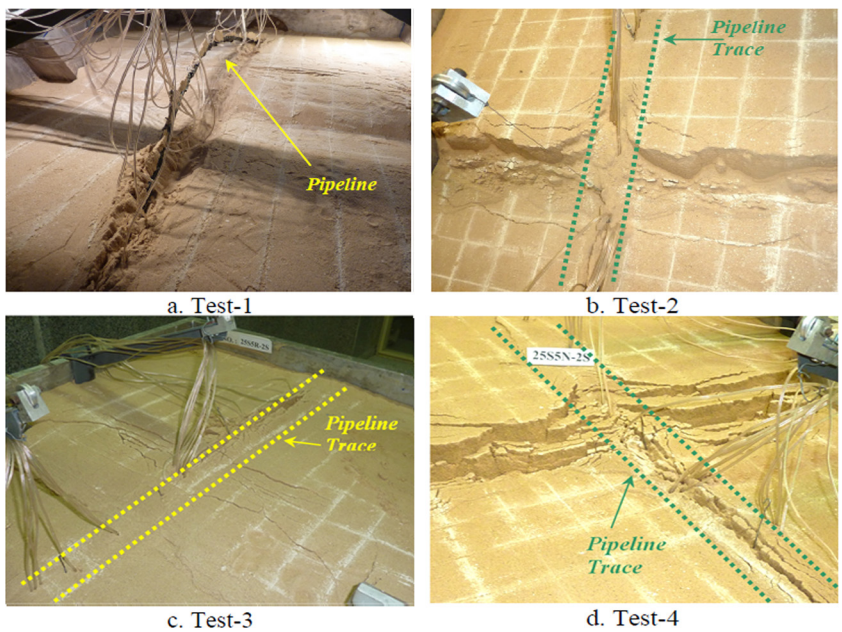

FIG. 8—*Post-test ground surface observations.*

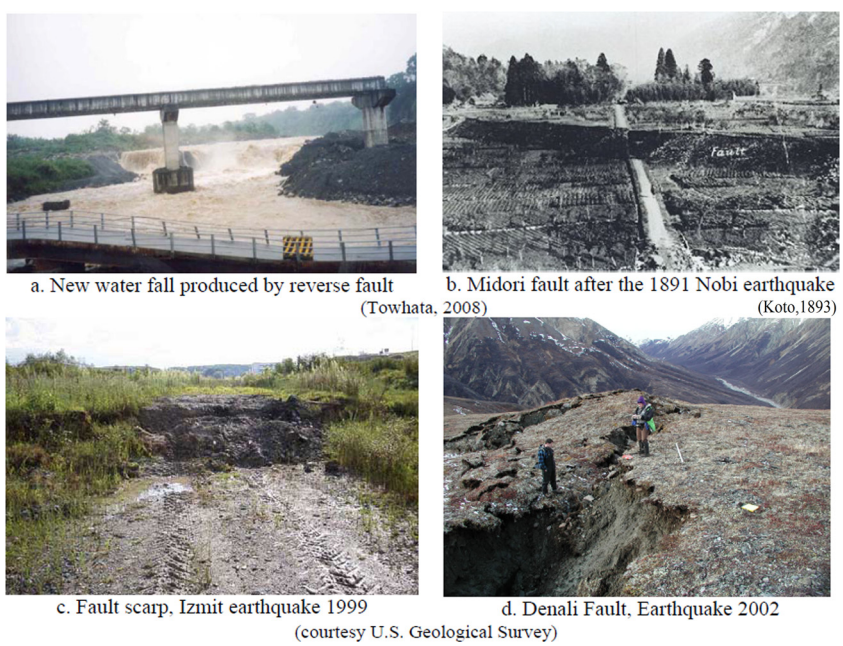

FIG. 9—*Post- faulting ground surface in earthquakes.*

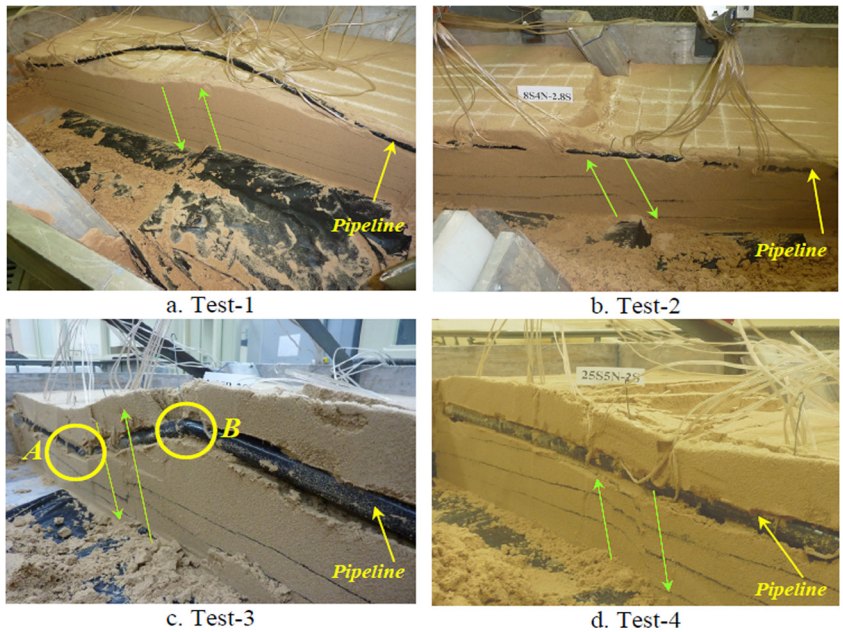

FIG. 10—*Post-test section observations.*

eight bearings and rails to minimize friction between the sliding surfaces (Fig. 6).

The hydraulic jack (element 7 in Fig. 4) has been installed horizontally under the soil container and exerts force on the wedge blunt end. A long, narrow hydraulic actuator is used to minimize the overall height of the system.

A set of linear guide way bearings and rails are used as a guide for the desired motion path (elements 3–4 in Fig. 4). The guide way bearings were designed to be installed on heavy load computer numerical control (CNC) machines. Each is capable of enduring a 33 kN load during normal operation. The moving section of the container can endure 120 kN of load, including the weight of the moving section itself. Mechanical failure of the bearings should occur at a much greater weight than the above-mentioned value by a safety factor of 4. This means that the simulator can operate at the specified acceleration (50 *g*) safely.

Hydraulic System

The specifications of the hydraulic system used for FSUT-RN60.8 is summarized in Table 2. The friction coefficient of the guide way bearings used is very low about 0.01 to 0.03. Thus, the system can project almost the entire horizontal actuator load in the desired direction multiplied by the projecting ratio.

Control System

The hydraulic system has a good capacity for accurate control of the motion and rate of motion. The control system of the FSUT-RN60.8 simulator only controls motion. The rate of motion is fixed and equal to the maximum available rate of the hydraulic system. Controlling the motion is accomplished manually using a control box. In addition, proximity limit switches were added at the end of the motion paths to limit the path of the actuator. At each end of the paths, one main and one backup limit switch were added.

Additional Features and Design Aspects

The edges of the box at the interface of the two portions of the soil container (element 5 in Fig. 4) were strengthened using aluminum plates with a thickness of 10 mm. Teflon sheets were added at the friction edges to reduce the friction and minimize soil loss. To obtain precise system, most of aluminum parts were cut using a CNC water-jet.

Test results from a model of a buried pipeline crossing normal and reverse faults were used to validate the usefulness of the FSUT-RN60.8 actuator design. This was done by observing the simulator performance and ground surface and pipe deformation due to faulting and comparing them with expected deformations. The results are presented below.

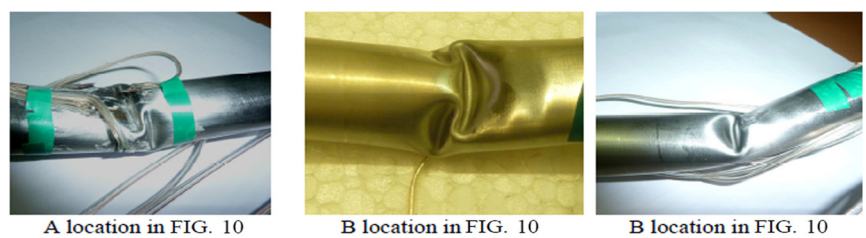

FIG. 11—*Wrinkling of pipe in test 3.*

Centrifuge Tests on Buried Pipe Model

Experimental Equipment

The Univ. of Tehran geotechnical centrifuge facility was manufactured by Actidyn Systems of France and the model is C67-2. The main characteristics of this centrifuge are shown in Table 3.

Buried Pipe Modeling

Research on the response of buried pipelines subject to faulting is currently being conducted at the Univ. of Tehran. The results of two centrifuge tests for normal faulting and two for reverse faulting using FSUT-RN60.8 are presented here. The scaling laws for centrifuge modeling are shown in Table 4 and a summary of the specifications for the centrifuge tests in prototype scale are presented in Table 5. All tests were conducted on a stainless steel 316 pipe with a pipe-fault intersection angle of 90° and a 60° fault dip angle at 40 *g* acceleration.

To realistically simulate the faulting effects on a pipeline using a centrifuge, the end connections of the pipe must be modeled suitably. Thus, a set of special connectors were designed to connect the test pipe to the simulator body to restrict pipe axial and bending deformation at the ends.

Two types of sensors were used to monitor the response of the pipeline subject to faulting: strain gauges and displacement transducers. The strain gauges were arranged at seven stations along the pipe in the longitudinal and circumferential directions and were wired as quarter bridges to capture the axial and bending strains separately. Displacement transducers measured the axial displacement of the pipe at the two ends, vertical displacement of the pipe in profile and fault displacement.

The soil used in this series of modeling was Firoozkouh-191 sand with 4%–5% moisture content. Figure 7 shows the grain size distribution curve of Firoozkouh-191. A comparison of test sand properties with Toyoura sand and Sengenyama sand is presented in Table 6. Tamping was used to compact the sand to prepare samples with 85% relative density. The steel tamper was 19.1 N in

FIG. 12—*Buckling of pipeline due to fault action, Manjil earthquake, Iran, 1990. (Towhata 2008).*

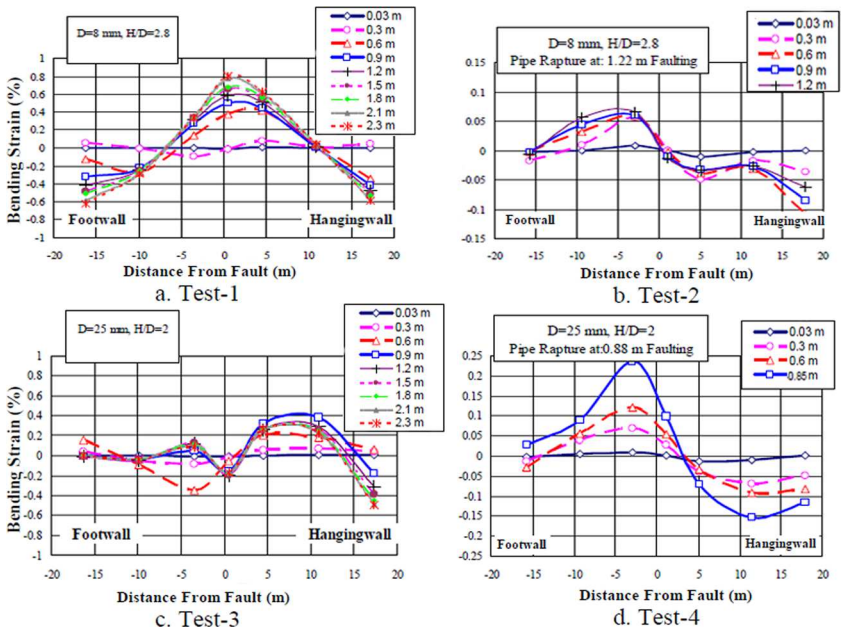

FIG. 13—*Bending strain during faulting.*

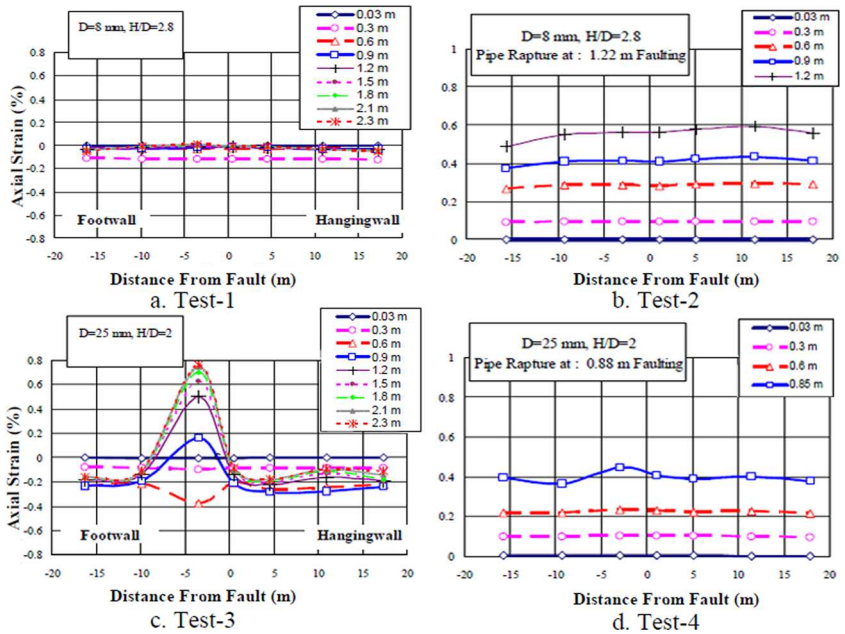

FIG. 14—*Axial strain during faulting.*

weight, 182 mm in width and 247 mm in length. The thickness of the soil layer at each compacted stage was 40 mm and the input energy for compaction was 425 J/m^2. Although the sand raining method is a more homogenous compaction method, tamping was suitable for this modeling because of the moisture and high relative density of the soil and the large deformation in the model (Byrne 2004).

Figures 8 and 10 show the ground surface and section deformations and pipe deformation. The deformations occurring at the ground surface during normal and reverse faulting are similar to natural ground surface at a fault. Figure 9 shows a sample of ground surface deformation in nature. As expected, during reverse faulting, soil to the left of the fault (foot wall side) appears relatively undisturbed, while the soil has been disturbed on the hanging wall side of the fault and a soil scarp was created along the surface trace of the fault similar to Figs. 8(*a*) and 8(*c*) and Figs. 9(*a*)–9(*c*). During normal faulting, the downward local slope occurred within the fault zone; thus, slumping along the cracks to form the small scarps should be apparent in Figs. 8(*b*) and 8(*d*) and Fig. 9(*d*). Figure 10 shows a section of soil deformation. The shear band of soil emerged and the propagation of reverse and normal faulting through soil could be investigated. The pattern of this shear zone was similar to that observed by Bransby et al. (2008), Ahmed et al. (2009), El Nahas et al. (2006) and Lee (2005).

The pipeline deformation in all tests was as expected and similar to natural events. In reverse faulting, compression force was exerted on the pipe and beam bucking of the pipeline occurred in the shallow buried depth condition [Fig. 10(*a*)]. When the pipeline was deeply embedded, it experienced local buckling and wrinkling [Figs. 10(*c*) and 11].

Beam buckling of pipes has been observed in two high pressure pipelines 219 mm in diameter during the 1979 Imperial Valley earthquake. Figure 12 shows beam buckling of a pipe in the 1990 Manjil earthquake in Iran. Wrinkling of a pipe can be found in the localized buckling of a liquid fuel pipeline in the 1991 Costa Rica earthquake caused by permanent ground deformation and in the wrinkling of water and gas pipelines in the 1994 Northridge event (O'Rourke and Liu 1999).

In normal faulting, tension force is exerted on a pipe and, at both shallow and deep burial depths, the pipeline experiences axial tension and rupture [Figs. 10(*b*) and 10(*d*)]. This behavior has been observed in the 1994 Northridge earthquake (O'Rourke and Liu 1999).

The results of bending and axial strain measurement of pipes during faulting are shown in Figs. 13–14. It was observed that, for beam buckling, axial strain on the pipe was negligible and bending strain was predominant. For the tensile deformation mode, axial strain was predominant and bending strain was less. In the wrinkling mode, both axial and bending strains are important because of the complicated deformation shown in Fig. 11.

Pipe axial and bending strain and profile deformation due to normal and reverse faulting is discussed in Rojhani et al. (2011a, 2011b, 2012). Ten centrifuge tests were performed to study pipeline behavior under normal and reverse faulting at shallow and deep burial depths using pipes with different diameters and thicknesses. The influence of faulting offset, burial depth and pipe diameter on the axial and bending strains of pipes and on ground soil failure and pipeline deformation were investigated. The centrifuge tests were performed to verify numerical and analytical research on pipeline response due to faulting.

Conclusion

In this paper, all available information on centrifuge fault simulators constructed worldwide was reviewed and their properties presented. A comparison of these five centrifuge fault simulators is presented in Table 7.

TABLE 7—*A comparison of all centrifuge fault simulators.*

Manufacturer:	RPI[a] (1st)	Waseda Univ.	RPI (2nd)	Univ. of Dundee	Univ. of Tehran
Material	n/a	steel, acrylic plate	aluminum	aluminum, steel, perspex	aluminum
Dimensions (mm)	1000 × 354 × 203	1200 × 800 × 450	1140 × 760 × 200	800 × 500 × 500	950 × 750 × 680
Faulting type	strike	normal, reverse	strike, normal, reverse	normal, reverse	normal, reverse
Dip. angle (deg.)	90°	45°	90°	60°	60°
Offset (mm)	±40	n/a	±40 (h) + 40 (n, r)	26.4 (n) 33 (r)	±40(n, r)
Actuator	hydraulic jack: 26.7 kN	double hydraulic jack: 2 MN	hydraulic jack: 26.7 kN	double hydraulic jack: 2 MN	hydraulic jack: 50 kN
Control system	motion, rate of movement	motion	motion, rate of movement	motion	motion
Development capability[b]	f: n/a d: not possible	f: not possible d: n/a	d: not possible	f: not possible d: possible	f: possible d: possible
Country, date	USA 2003	Japan 2005	USA 2006	UK 2006	Iran 2010

[a] Rensselaer Polytechnic Institute.
[b] F = fault; D = dip angle

An advanced fault simulator (FSUT-RN60.8) was successfully designed and manufactured at the Univ. of Tehran that simulates normal and reverse faulting. The FSUT-RN60.8 simulator could be developed to simulate strike-slip and oblique faulting. The simulation of other fault dip angles is readily possible by changing out parts of the simulator. All properties and details of this simulator are described.

The main advantage of FSUT-RN60.8 is the moving wedge mechanism which has high stability, a low capacity actuator requirement and suitable performance.

The operation of this simulator was successfully tested and was in accordance with expectations. The first series of tests was the centrifuge modeling of a buried pipeline affected by normal and reverse faulting with a dip angle of 60°. The ground and pipe deformations were in good agreement with observed natural events.

Acknowledgments

This research was sponsored by the Faculty of Engineering of the University of Tehran. This support is gratefully acknowledged. The writers wish to thank the staff of the Soil Mechanics and Physical Modeling Laboratory, especially Mr. Salimi and Mr. Shakori. The assistance of Mr. Pirnazari in equipping the laboratory is greatly appreciated.

References

Ahmed, W. and Bransby, M. F., 2009, "Interaction of Shallow Foundations with Reverse Faults," *J. Geotech. Geoenviron. Eng.*, Vol. 135, No. 7, pp. 914–924.

Bransby, M. F., Davies, M. C. R., and El Nahas, A., 2008, "Centrifuge Modeling of Normal Fault-Foundation Interaction," *Bull. Earthquake Eng.*, Vol. 6, pp. 585–605.

Byrne, P. M., Park, S. S., Beaty, M., Sharp, M., Gonzalez, L., and Abdoun, T., 2004, "Numerical Modeling of Liquefaction and Comparison with Centrifuge Tests," *Can. Geotech. J.*, Vol. 41, pp. 193–211.

Choo, Y. W., Abdoun, T. H., O'Rourke, M. J., and Ha, D., 2007, "Remediation for Buried Pipeline Systems under Permanent Ground Deformation," *Soil Dyn. Earthquake Eng.*, doi:10.1016/j.soildyn.2007.04.002.

El Nahas, A., Bransby, M. F., and Davies, M. C. R., 2006, "Centrifuge Modeling of the Interaction between Normal Fault Rupture and Rigid, Strong Raft Foundations," *Proceedings, International Conference on Physical Modeling in Geotechnics*, Ng et al, Eds., Taylor & Francis Group PLC, London, Vol. 1, pp. 337–342.

Ghalandarzadeh, A., 1997, "Shaking Table Tests on Seismic Displacement of Water-Front Structures," Ph.D. Dissertation, Univ. of Tokyo, Japan.

Ha, D., Abdoun, T., O'Rourke, M., Van Laak, P., O'Rourke, T., and Stewart, H., 2006, "Split-Containers for Centrifuge Modeling of Permanent Ground Deformation Effects on Buried Pipeline Systems," *Proceedings of the Sixth International Conference on Physical Modeling in Geotechnics*, Hong Kong, pp. 729–34.

Lee, J. W., 2005, "Study on Earthquake Fault Rupture Propagation through Sandy Soil Deposit," Ph.D. thesis, Waseda Univ., Tokyo.

Lee, J. W. and Hamada, M., 2005, "An Experimental Study on Earthquake Fault Rupture Propagation through a Sandy Soil Deposit," *Struct. Eng./Earthquake Eng.*, Vol. 22, No. 1, pp. 1s–13s.

O'Rourke, M. and Liu, X., 1999, *Response of Buried Pipelines Subject to Earthquake Effects*, Multidisciplinary Center for Earthquake Engineering Research (MCEER), Monograph Series, 250 pp.

O'Rourke, M., Vikram, G., and Abdoun, T., 2003, "Centrifuge Modeling of Buried Pipelines," *Proceedings of the Sixth U.S. Conference and Workshop on Lifeline Earthquake Engineering*, Long Beach, CA, pp. 757–768.

Rojhani, M., Moradi, M., Galandarzadeh, A., and Takada, S., 2011a, "Centrifuge modeling of buried pipelines response due

to reverse faulting," *Proceedings, 5th International Conference on Earthquake Geotechnical Engineering*, Santiago, Chile, Paper No. CMBRO.

Rojhani, M., Moradi, M., Galandarzadeh, A., and Takada, S., 2011b, "Centrifuge modeling of buried pipelines response due to normal faulting," *Proceedings, 14th Asian Regional Conference on Soil Mechanics and Geotechnical Engineering*, Hong Kong, China, Paper No. 188.

Rojhani, M., Moradi, M., Galandarzadeh, A., and Takada, S., 2012, "Centrifuge Modeling of Buried Continuous Pipelines Subjected to Reverse Faulting," *Can. Geotech. J.*, Vol. 49, No. 6, 2012, pp. 659–670.

Simpson, B. and Tatsuoka, F., 2008, "Geotechnics: The Next 60 Years," *Geotechnique*, Vol. 58, No. 5, pp. 357–368.

Towhata, I., 2008, *Geotechnical Earthquake Engineering*, Springer, Verlag Berlin Heidelberg.